Spherical proportional counters; development, improvement and understanding

A. Brossard

Version of Record: https://www.sciencedirect.com/science/article/pii/S0168900218315833
Manuscript_f8319405929d7d61cffb8ccf7fe23181

NIMA POST-PROCESS BANNER TO BE REMOVED AFTER FINAL ACCEPTANCE

Spherical Proportional Counters; development, improvement and understanding

A. Brossard[a,b,*], on behalf of the NEWS-G collaboration (news-g.org)

[a]*Department of Physics, Engineering Physics & Astronomy, Queen's University, Kingston, Ontario k7L 3N6, Canada*
[b]*IRFU, CEA, Université Paris-Saclay, F-91191 Gif-sur-Yvette, France*

Abstract

The New Experiments With Spheres-Gas (NEWS-G) collaboration uses spherical proportional counters (SPCs) filled with light noble gases for rare event detection. SPCs are a novel technology that have many appealing features for particle detection including sub-keV thresholds, single electron sensitivity, excellent energy resolution and flexibility in gas choice. In this paper, studies conducted at Queen's University, focusing on the understanding, monitoring and improvement of the detector response will be presented. The detector consists of a 30 cm diameter sphere with a 2 mm anode at the center. With this set-up, we perform precision measurements with a UV laser and radioactive sources that encompass a wide range of fundamental characteristics of the detector.

Keywords: Spherical Proportional Counter, Single electron detection, Gas Detectors

1. Introduction

The Spherical Proportional Counter (SPC) is a novel concept developed in 2006 at the CEA Saclay by I. Giomataris [1]. Its low intrinsic electronic noise in addition to its large amplification allows for a very low energy threshold, down to single electron detection. It's unique characteristics make SPCs competitive detectors for rare event detection applications such as dark matter and neutrino physics. The NEWS-G experiment primarily focuses on the search for light dark matter. The collaboration recently published the first results obtained with a 60 cm diameter SPC, SEDINE, operated at the Laboratoire Souterrain de Modane [2]. The competitive constraints are promising for the next phase of the experiment: a 140 cm diameter sphere made of selected radio-pure material and placed inside an enhanced shielding, to be installed at SNOLAB during spring 2019.

In addition to these hardware improvements, the next detector generation will benefit from an intensive study of the electric field and the development of new methods of calibration which greatly improved our understanding of the detector response. This proceeding will first overview the detector principle, then focus on the development of the sensor. Finally, the latest calibration, with sensitivity to single electrons using a solid state laser, will be presented. These studies were done with a 30 cm diameter sphere operating at Queen's University, filled with 500 $mbar$ of gas mixture made of 98% of Ar and 2% of CH_4.

2. Operating principle of the detector

Figure 1 depicts an SPC and its operation. The detector consists of a grounded, metallic spherical vessel filled with gas. The anode is a small ball made of metallic or resistive material, placed at the center of the sphere and supported by a grounded metallic rod, through which the high voltage is applied. In an ideal SPC, the electric field depends on the anode radius r_2, cathode radius r_1, anode voltage V_0 and radial distance r from the anode. It is defined by:

$$E(r) = \frac{V_0}{r^2}\frac{r_2 r_1}{r_1 - r_2} \quad (1)$$

The electric field in the detector rapidly decreases with the square of the inverse distance from the center. This configuration divides the detector volume into two regions; the amplification region, less than 1mm around the anode, and the

*Alexis Brossard
Email address: alexis.brossard@queensu.ca (on behalf of the NEWS-G collaboration (news-g.org))

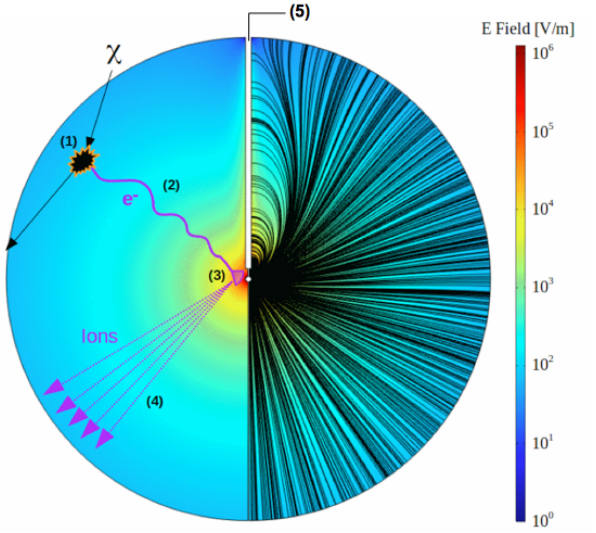

Figure 1: Schematic view of the Spherical Proportional Counter and detection principle.

drift region. When particles interact in the gas volume, they ionize some gas, inducing the emission of primary electron (1). Under the influence of the electric field, the primary electrons drift toward the anode at the center of the sphere (2). The typical drift time varies from μs to ms depending on gas pressure and composition. When primary electrons reach the amplification region, the strong electric field gives them a sufficient kinetic energy to produce secondary ion-electron pairs, creating a charges avalanche (3). The signal is then induced by the motion of secondary ion toward the cathode (4). Finally, the signal is extracted from the high voltage wire through a capacitor, amplified by a charge amplifier (5), with time constants from tens to hundreds of μs.

It is possible to extract two main observables from the recorded pulses; theirs amplitudes and rise times. The amplitude is directly dependent on the energy of the deposition. The rise time of the recorded pulses is correlated to the spatial distribution of the energy deposition. Energy deposition along a track leads to a large rise time defined by the difference of arrival time of primary electrons on the anode. For point like energy depositions, the rise time is defined by the diffusion of primary electrons which is correlated to the drifting distance.

3. Sensor development

The high voltage for the anode is provided by a wire encased in a grounded supporting rod. This breaks the symmetry of the electric field. As shown on Figure 1, (right half of the sphere) the electric field is not isotropic. More precisely, the anisotropy of the electric field in the amplification region (Figure 2) induces a dependence of the gain on the arrival angle of the primary electrons.

Having a simple sensor also limits the voltage that can be applied on the anode before electric discharge occurs between the ball and the rod. A solution to these issues is the use of

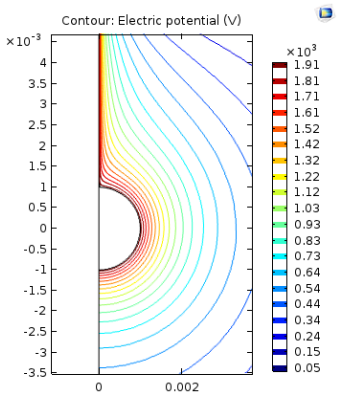

Figure 2: Electric field norm in the amplification region around a 2 mm diameter anode.

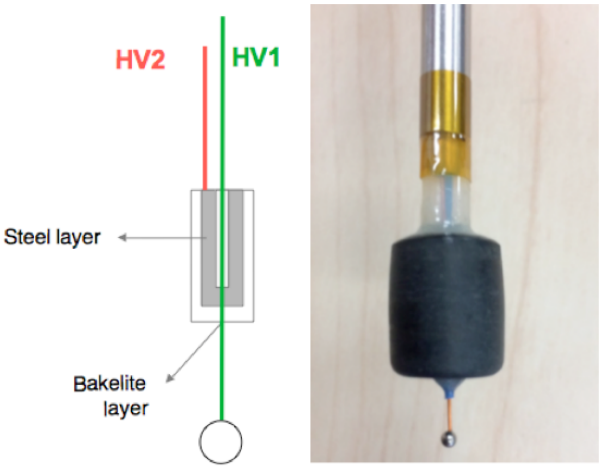

Figure 3: Left: Schematic view of the bakelite sensor with $HV1$ applied on the anode and $HV2$ on the a steel layer inside bakelite. Roght: Picture of a 2 mm diameter anode with bakelite umbrella used at queen's university.

resistive material for a field corrector, a so called "umbrella". The umbrella is installed between the ball and the anode. A secondary voltage, $HV2$, can be applied on the umbrella to correct the effects of the anisotropy of the electric field. The umbrella is made of resistive material to allow the application of a voltage on its surface and prevent from electric discharge with the anode. Figure 3 shows a bakelite umbrella. The resistivity of bakelite has been measured to be on the order of $10^{12}\,\Omega \cdot cm$.

Two strategies can be employed to improve the detector response. The first one is to apply a positive or null HV2, close to the anode to make the electric field isotropic in the amplification region. The applied voltage and the anode to umbrella distance can be tuned to obtain the best response. The second strategy is to apply a negative voltage on the umbrella to neutralize the low gain region. Primary electrons from the whole detector volume will drift toward the lower half of the sensor where the electric field in the avalanche region is isotropic. The results obtained with this second strategy are presented below.

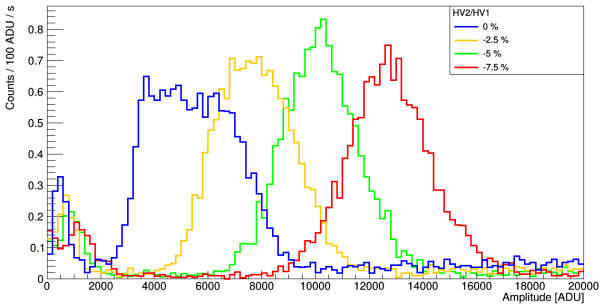

Figure 4: Effect of the second voltage applied on the umbrella. The voltage applied on the anode was kept constant at 2000 V. The peak is due to the decay of ^{37}Ar releasing 2.82 keV X-rays

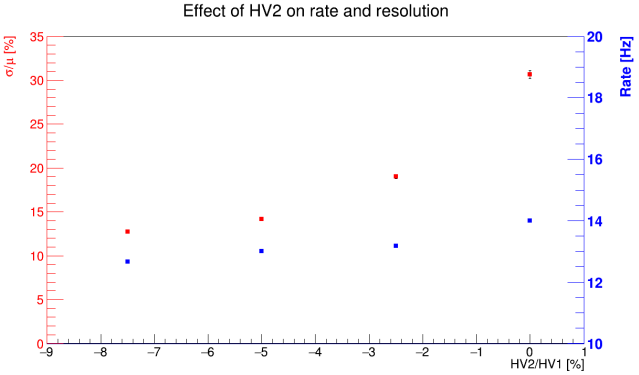

Figure 5: Effect of HV2 on the resolution (red) and rate (blue) of the 2.82 keV peak of ^{37}Ar. Applying a negative HV2 improves the resolution of the detector without significantly affecting the active volume the detector.

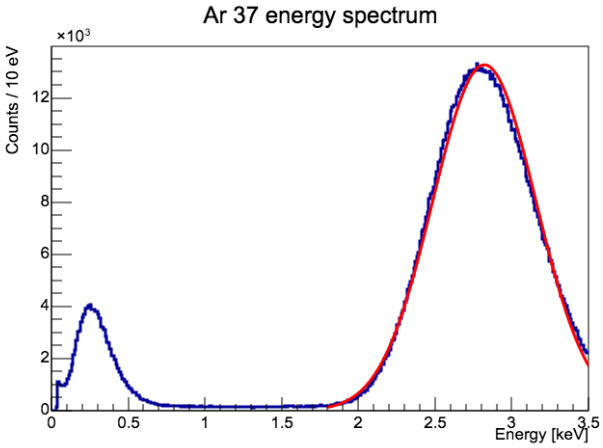

Figure 6: Energy spectrum of ^{37}Ar. The gaussian fit on the 2.82keV peak has a resolution of σ/μ = 12%

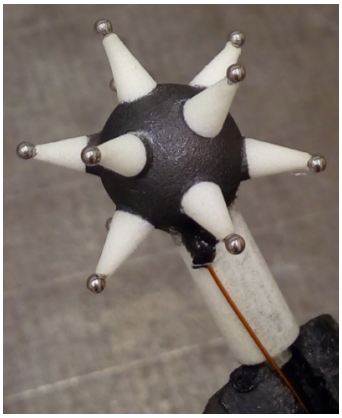

Figure 7: Picture of a multi-branch "Achinos" sensor.

Figure 4 shows the effect of the voltage applied on the umbrella. These measurements were done with ^{37}Ar, a radioactive gas which decays by electron capture. Capture from the K-shell and L-shell release 2.82 keV and 270 eV X-rays respectively. The sphere was filled with 500 $mbar$ of gas mixture made of 98% of Ar and 2% of CH_4. The voltage $HV1$ applied on the anode was +2000 V and four voltages were tested on the umbrella.

When we decrease $HV2$, keeping $HV1$ constant, the peak due to capture from K-shell is shifted towards larger amplitude, showing an increase of the detector gain. This decrease of HV2 also improves the detector energy resolution. For $HV2 = 0V$, the recorded spectrum does not exhibit a gaussian shape. By applying a negative HV2, in order to obtain a ratio $HV1/HV2$ equal to -2.5%,-5% and -7.5% the gaussian fits on the yellow, green and red curves show a resolution of 18.5%, 14.2% and 12.7% respectively. These results confirm an improvement of the homogeneity of the gain of the detector for events distributed in its whole volume.

Figure 5 shows the effect of HV2 on the detector resolution and the event rate. A reasonable negative value of HV2, higher than -8% of HV1, strongly improve the detector resolution with a very small loss of sensitive volume.

Figure 6 shows data where the voltage applied on the bakelite umbrella was $-120\,V$ and $+2020\,V$ was applied on the 2 mm anode. The fit of the 2.82 keV peak has a resolution σ/μ = 12% where the best resolution achievable taking into account the statistic of primary electron emission and Townsend avalanche is about 11%. The 270 eV peak from L-shell electronic capture is clearly visible on the left of the spectrum showing the capability of SPCs for $sub-keV$ detection.

Large future detectors will require new sensor technologies to still allow for single electron detection. The size of the anode and the value of the high voltage need to reach a compromise between the amplification and the strength of the electric field. These two imperatives lead to a conflict for large scale detectors. To avoid electron attachment, a strong field is needed, requiring a large anode. In the other hand, the high gain needed for $sub-keV$ threshold demands a small anode. The collaboration is studying the behaviour of multi-branch electrods seen on figure 7. This promising geometry has the same effect as a large ball at long distance, the value of the electric field being defined by the size of the whole structure, providing a good drift field. At the same time, the small balls ensure a good amplification at short distance [3].

4. Single electron response

The main goal of the single electron calibration is the parametrization of the theoretically motivated Polya distribution describing the gain of the detector. Specifically, it describes the number of ion-electron pairs produced by an avalanche induced by one electron. [5]

$$P\left(\frac{N}{<N>}\right) = \frac{N}{<N>} \times \frac{(1+\theta)^{(1+\theta)}}{\Gamma(1+\theta)} \frac{N}{<N>}^{\theta} exp\left(-(1+\theta)\frac{N}{<N>}\right) \quad (2)$$

The detector response to single electrons has been studied using a solid state laser. A $213\,nm$ light beam is splitted and sent through an optic fibre to a photo-detector and inside the sphere. Primary electrons are extracted from the sphere's inner surface by the photoelectric effect. This method of calibration allows us to perform several measurement such as drift time, diffusion time and attachment rate of primary electrons. The laser is also used to monitor the stability of the detector with time.

Figure 8 presents the fit of laser data taken by triggering on the photo-detector. With a strong enough attenuation of the light beam, the number of extracted electron follows a Poisson distribution with less than one electron expected. The recorded events are noise fluctuation when no primary electrons are extracted, thus the gaussian shape on the left of the spectrum centred at $0\,ADU$. The tail at higher amplitude is the contribution of events with one or two primary electrons emitted. The fit of the recorded spectrum allows us to determine the mean number of primary electrons emitted ($\mu = 0.08$), the mean gain ($< G >= 41.6\,ADU/e^{-}$), and the baseline resolution ($\sigma = 4.3\,ADU$). Sensitivity to single electrons allows us to determine the parameter of the θ parameter of the Polya distribution. For the tested conditions of gas and voltage, this parameter is close to 0.

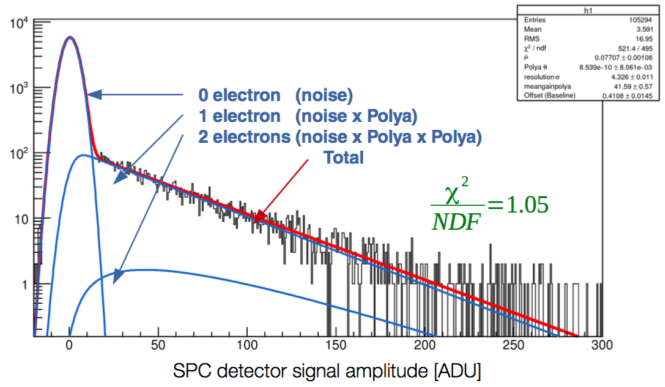

Figure 8: Data taken with solid state laser. The fit of the data (red) allows us to determine the mean number of primary electrons extracted from the sphere surface ($\mu = 0.08$). The blue curves represent the contribution of events for which 0, 1 or 2 primary electrons were extracted.

Figure 9 shows the mean number of primary electrons vs the amplitude of pulses recorded by the photo-detector. μ is the only parameter of the fit that depends on the intensity of the laser pulses. The linear relationship between these two variables demonstrates the accuracy of a Poisson distribution for the number of extracted primary electron.

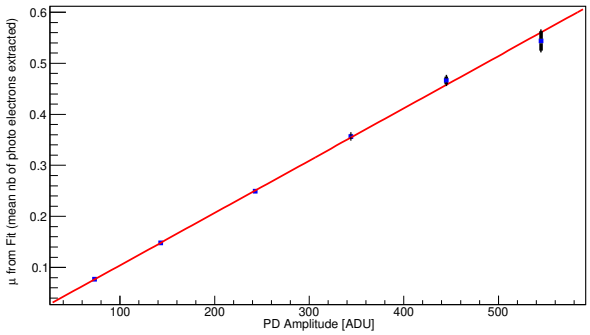

Figure 9: Mean number of primary electron extracted from the sphere surface.

5. Conclusion

SPCs have already shown their potential for dark matter detection with the SEDINE detector. New calibration methods confirm the ability of the detector to measure single electrons. The excellent fit of laser data shows a good understanding of the detector from energy deposition to signal formation. This improved understanding will us allow to reach a greater sensitivity to dark matter particle with an SPC et SNOLAB.

Acknowledgments

The presented studies have been made possible with the use of ^{37}Ar. The author thanks the Royal Military College of Canada, where the source is produced by irradiation of CaO with a SLOWPOKE-2 reactor [4]. The author thanks the Queen's University and the Commissariat à l'Energie Atomique.

References

[1] Giomataris I et al. 2008 JINST 3 P09007 (Preprint 0807.2802)
[2] Arnaud Q et al. (NEWS-G) 2018 Astropart. Phys. 97 54–62 (Preprint 1706.04934)
[3] A. Giganon *et al.*, JINST **12**, no. 12, P12031 (2017) doi:10.1088/1748-0221/12/12/P12031 [arXiv:1707.09254 [physics.ins-det]].
[4] D.G. Kelly et al. The Facile Production of Ar-37 Using a Thermal Neutron Reactor Flux, Journal of Radioanalytical and Nuclear Chemistry, Submitted April 2018.
[5] G.D. Alkhazov, Nucl. Instrum. Methods 89 (1970) 155 – 165. doi:10.1016/0029-554X(70)90818-9.